



## Article

# Influence of the Tissue Collection Procedure on the Adipogenic Differentiation of Human Stem Cells: Ischemic versus Well-Vascularized Adipose Tissue

Pallabi Pal <sup>1,†</sup> , Abelardo Medina <sup>2,†</sup>, Sheetal Chowdhury <sup>1</sup> , Courtney A. Cates <sup>1</sup>, Ratna Bollavarapu <sup>1</sup>, Jon M. Person <sup>3</sup>, Benjamin McIntyre <sup>2</sup>, Joshua S. Speed <sup>4</sup> and Amol V. Janorkar <sup>1,\*</sup>

<sup>1</sup> Department of Biomedical Materials Science, School of Dentistry, University of Mississippi Medical Center, 2500 N State Street, Jackson, MS 39216, USA

<sup>2</sup> Division of Plastic Surgery, Department of Surgery, University of Mississippi Medical Center, 2500 N State Street, Jackson, MS 39216, USA

<sup>3</sup> Cancer Institute, University of Mississippi Medical Center, 2500 N State Street, Jackson, MS 39216, USA

<sup>4</sup> Department of Physiology and Biophysics, University of Mississippi Medical Center, 2500 N State Street, Jackson, MS 39216, USA

\* Correspondence: ajanorkar@umc.edu; Tel.: +1-601-984-6170

† These authors contributed equally to this work.

**Abstract:** Clinical and basic science applications using adipose-derived stem cells (ADSCs) are gaining popularity. The current adipose tissue harvesting procedures introduce nonphysiological conditions, which may affect the overall performance of the isolated ADSCs. In this study, we elucidate the differences between ADSCs isolated from adipose tissues harvested within the first 5 min of the initial surgical incision (well-vascularized, nonpremedicated condition) versus those isolated from adipose tissues subjected to medications and deprived of blood supply during elective free flap procedures (ischemic condition). ADSCs isolated from well-vascularized and ischemic tissues positively immunostained for several standard stem cell markers. Interestingly, the percent change in the CD36 expression for ADSCs isolated from ischemic versus well-vascularized tissue was significantly lower in males than females ( $p < 0.05$ ). Upon differentiation and maturation to adipocytes, spheroids formed using ADSCs isolated from ischemic adipose tissue had lower triglyceride content compared to those formed using ADSCs isolated from the well-vascularized tissue ( $p < 0.05$ ). These results indicate that ADSCs isolated from ischemic tissue either fail to uptake fatty acids or fail to efficiently convert those fatty acids into triglycerides. Therefore, more robust ADSCs suitable to establish in vitro adipose tissue models can be obtained by harvesting well-vascularized and nonpremedicated adipose tissues.

**Keywords:** flow cytometry; CD36; 3D spheroid; triglyceride; adipose tissue



**Citation:** Pal, P.; Medina, A.; Chowdhury, S.; Cates, C.A.; Bollavarapu, R.; Person, J.M.; McIntyre, B.; Speed, J.S.; Janorkar, A.V. Influence of the Tissue Collection Procedure on the Adipogenic Differentiation of Human Stem Cells: Ischemic versus Well-Vascularized Adipose Tissue. *Biomedicines* **2024**, *12*, 997. <https://doi.org/10.3390/biomedicines12050997>

Academic Editors: Sofia M. Calado and Álvaro Plaza Reyes

Received: 22 March 2024

Revised: 26 April 2024

Accepted: 28 April 2024

Published: 1 May 2024



**Copyright:** © 2024 by the authors. Licensee MDPI, Basel, Switzerland. This article is an open access article distributed under the terms and conditions of the Creative Commons Attribution (CC BY) license (<https://creativecommons.org/licenses/by/4.0/>).

## 1. Introduction

The occurrence of obesity has steadily increased in recent decades and contributed to several diseases like type-2 diabetes, hypertension, and coronary heart disease in both men and women of all ages, races, and ethnicities [1]. By 2030, it is projected that approximately 60% of adults around the world will be overweight or obese [2]. In individuals with obesity, the adipose tissue is the largest endocrine organ because it can account for almost half the body weight [3]. Thus, in such individuals, minor metabolic changes in adipose tissue can impact the function of the entire body. Better knowledge of the adipose tissue structure and function is therefore critical to develop novel strategies that would work at the cellular level and reduce the deleterious effects of obesity. Mesenchymal stem cells are commonly used for adipose-related in vitro studies. Within this cell category, adipose-derived stem cells (ADSCs) are becoming popular as a result of their easy isolation from the adipose stromal vascular fraction (SVF), ease of adipose tissue accessibility, stem cell quality, and

pluripotency. ADSCs also possess *in vitro* proliferative potential along with multilineage differentiation capacity [4–6].

The use of ADSCs in different *in vivo* and clinical settings is in rapid expansion. For instance, the application of ADSCs in *in vivo* animal models stimulates neovascularization in soft tissue transfer procedures [7,8]. ADSCs may have an important role in chimeric or prefabricated flaps for complex or three-dimensional surgical reconstructions in trauma patients or after cancer excision. In addition, ADSCs are thought to reduce ischemia/reperfusion injury, which may positively impact the management of burn injuries, acute kidney injuries, myocardial infarction, chronic nonhealing wounds (e.g., diabetic ulcers), and pressure ulcers and ischemic limbs [9–13].

Even though the clinical applications of ADSCs appear to be beneficial and safe, there is no current consensus on optimization of specimen collection and ADSC isolation or the appropriate dose, administration route, and treatment duration [14]. Rodbell and colleagues pioneered the technique to isolate ADSCs from rat epididymal fat [15]. The initial isolation procedure has undergone various modifications for isolation from human tissue. Current methods of cell isolation rely on collagenase digestion of the tissue to loosen the cells from the extracellular matrix and selecting the plastic-adherent ADSCs [16]. There is no definitive data on whether to use freshly isolated autologous SVF cells or *in vitro* expanded ADSCs because freshly isolated ADSCs and cultured ADSCs do not share the same phenotype and functions [17–22]. In addition to the physiological factors, numerous nonphysiological conditions are experienced during the current fat tissue harvesting procedures of abdominoplasty and liposuction that may affect the recruitment, proliferative potential, gene expression, and final reprogramming capability of the ADSCs. These factors include the considerable time of ischemia and hypoxia along with the effect of local medications (i.e., epinephrine, lidocaine, sodium bicarbonate, etc.). For instance, lidocaine has deleterious effects on ADSCs in a dose- and time-dependent manner regarding cell viability, proliferative capacity, and gene expression [23–25].

In this study, we aim to assess the differences between the stem cell populations isolated from adipose tissues harvested using the current method (which yields ischemic and chemically manipulated tissue samples) and a novel well-vascularized, nonchemically treated tissue harvest procedure. We hypothesized that an ADSC population obtained from “nonpremedicated and well-vascularized” adipose tissue has the potential to create more robust cell subsets in terms of lineage commitment (e.g., adipogenesis) and generate better *in vitro* culture models. This novel approach will determine how crucial procedural steps in clinical operational settings may negatively impact the current practice of ADSCs harvesting. To show the differences in marker-profile and differentiation-potential between ADSCs isolated from well-vascularized and ischemic samples, we have focused on the adipogenic differentiation. Current anti-obesity drugs mainly act like an appetite suppressor, have limited efficacy, and often come with significant side effects. To address this gap, researchers are turning to *in vitro* adipose culture models [26–29]. The evaluation of the effect of ADSCs origin would offer insights into adipocyte behavior under fat-laden conditions, crucial for developing more effective obesity treatments and combating its cardiovascular consequences.

## 2. Materials and Methods

### 2.1. Sample Collection

Adipose tissue samples were harvested from adult male and female patients (n = 4 per group) undergoing anterolateral thigh (ALT) free flap surgeries (Figure 1). The donor characteristics are summarized in Table 1. All donors had no other comorbidities. The following samples were collected as approved by the University of Mississippi Medical Center Institutional Review Board (Approval # 2012-0004, Initial approval: 16 March 2012, Most recent annual approval: 24 June 2023):

1. Well-vascularized tissue: Adipose tissues were obtained at the beginning of the surgery (within the first 5 min of the initial surgical incision). These tissue samples were in a well-vascularized, nonpremedicated condition.
2. Ischemic tissue: Adipose tissues were obtained after the ALT flaps were fully harvested from the more distal part of the flaps where the blood supply was considered deprived.

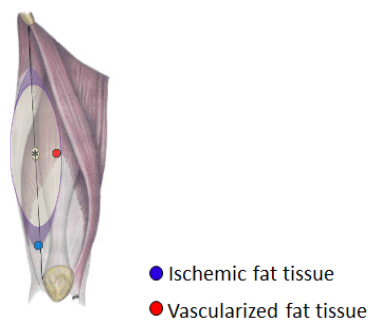


**Figure 1.** Site of adipose tissue collection during anterolateral thigh (ALT) free flap surgery. Well-vascularized tissue was harvested within the first 5 min of the initial surgical incision while ischemic tissue was harvested from the more distal part of the flaps.

**Table 1.** Characteristics of patients from whom the ADSCs were isolated. C = Caucasian, AA = African American or Black.

Patient #	Gender	Age	BMI	Race
1	Female	68	28.6	C
2	Female	74	30.9	C
3	Female	65	27.0	AA
4	Female	40	28.0	AA
5	Male	69	33.7	C
6	Male	58	33.3	C
7	Male	56	21.6	AA
8	Male	40	35.9	AA

## 2.2. ADSC Isolation and Maintenance

For the vascularized tissues, samples were collected and placed in the media immediately and transported to the laboratory for isolation. The ischemic tissue samples were obtained after the surgeries were complete (typically, 3 h after the vascularized sample collection). The ADSC isolation process lasts between 3 and 4 h. Consequently, the ischemic tissues experienced a total of 6–7 h of ischemic conditions. ADSCs isolated from the adipose tissues were cultured and differentiated following Turner et al. [6]. Briefly, the tissue was minced into small sections, digested in collagenase I ( $1 \text{ g L}^{-1}$  in PBS) for 45 min at  $37^\circ\text{C}$  and filtered through a  $100 \mu\text{M}$  cell strainer. Pre-adipocyte media (1:1 DMEM:Ham's F12 with 10% calf serum) was added to the filtrate and centrifuged at  $1200 \times g$  for 5 min. The cell pellet was suspended in an erythrocyte lysis buffer for 10 min before centrifugation at  $1200 \times g$  for 5 min. The pellet was resuspended in pre-adipocyte media and filtered through a  $70 \mu\text{M}$  cell strainer. The filtrate containing SVF cells including ADSCs were cultured on tissue culture polystyrene dishes in pre-adipocyte media at  $37^\circ\text{C}$  and 5%  $\text{CO}_2$ , with media changes every 2–3 days. Cells were used for experiments between their third and sixth passage.

## 2.3. Cell Morphology

The morphology of ADSCs isolated from well-vascularized and ischemic tissues were examined using an Olympus IX 81 optical microscope. Images were captured at three different locations per culture plate using a Hamamatsu digital camera connected

to Slidebook image acquisition software (Slidebook 4.2.0.10, Olympus, Center Valley, PA, USA).

#### 2.4. Flow Cytometry

Flow cytometry measurements were conducted using mouse antihuman fluorochrome-conjugated monoclonal antibodies of CD29, CD31, CD36, CD44, CD59, CD90, CD105, CD106, CD117, and CD271. All antibodies except CD90 were purchased from BD Pharmingen™, while CD90 was purchased from eBioscience™, Invitrogen. Briefly, 100,000 ADSCs were washed twice with 1× mouse serum, resuspended in 1× mouse serum, and fluorochrome-conjugated antibodies were added per manufacturers' protocols. After 30 min incubation, the cell–antibody conjugates were washed twice with 1× mouse serum and analyzed with a multicolor Beckman Coulter Gallios, B5-R1 configuration flow cytometer and Kaluza v2.1 software. Control gates were set with matched labeled isotype control IgG antibodies.

#### 2.5. Coating Tissue Culture Plates

Elastin-like polypeptide (ELP) was produced in-house using genetically engineered *Escherichia coli* and conjugated with polyethyleneimine (PEI) following Turner et al. [30]. Then, 24-well tissue culture polystyrene plates were coated by adding 200 µL of 5 mol% ELP-PEI solution in deionized water (5 g L<sup>-1</sup>) per well and dried at 37 °C for 48 h.

#### 2.6. ADSC Spheroid Formation, Differentiation, and Maturation

Fifty thousand ADSCs per well were seeded on the ELP-PEI coated 24-well plate and incubated at 37 °C, 5% CO<sub>2</sub> for a 72 h period undisturbed to allow spheroid formation. ADSCs were then supplemented with differentiation media (1:1 DMEM:Ham's F12 media with 1 µM dexamethasone, 0.5 mM IBMX, 0.1 U mL<sup>-1</sup> insulin, 1 µM indomethacin, and 100 U penicillin/100 µg streptomycin mL<sup>-1</sup>) for 72 h [6]. After differentiation, cells were exposed to maturation media (1:1 DMEM:Ham's F12 media with 10% fetal bovine serum, 0.2 U mL<sup>-1</sup> insulin, 100 U penicillin/100 µg streptomycin mL<sup>-1</sup>) for up to 10 days. The cells were formed into spheroids and then differentiated into adipogenic lineage for two main reasons. First, this method avoids an extra trypsinization step required if the cells were to be differentiated first as a monolayer and then plated to form spheroids. Second, spheroid formation facilitates cell–cell interactions and cell–matrix communication. This architecture mimics the three-dimensional microenvironment found in vivo. Our prior work has shown that the spheroid culture can promote superior cell differentiation [6,30].

#### 2.7. Measurement of Spheroid Size

Spheroids were imaged using an Olympus IX 81 optical microscope with a Hamamatsu digital camera and Slidebook image acquisition software (Slidebook 4.2.0.10, Olympus, Center Valley, PA, USA). ImageJ digital analysis software (<https://imagej.net/ij>, accessed on 22 January 2024) was used to measure the spheroid sizes on a minimum of 50 spheroids per condition.

#### 2.8. Biochemical Measurements

ADSC spheroids were collected after 3 days in differentiation media (i.e., day 0 of maturation media, M0) and 10 days in maturation media (M10) by aspiration and centrifuged for 2 min at 2000 rpm. Spheroids were then suspended in PBS and lysed using a Branson Digital Sonifier 450 (Danbury, CT, USA) for 1 min at 10% amplitude. All assays were performed in triplicates according to manufactures' protocols. DNA and protein content were evaluated using the CyQuant DNA assay and BCA total protein assay, respectively (ThermoFisher Scientific, Waltham, MA, USA). Intracellular triglyceride (TG) content was measured using triglyceride and glycerol kit (Sigma-Aldrich, St. Louis, MO, USA).

### 2.9. Statistical Analysis

One-way ANOVA with the Games–Howell post hoc test for unequal variances was used for statistical data analysis. Data are shown as mean  $\pm$  95% confidence interval. Values with  $p \leq 0.05$  were deemed statistically significant.

## 3. Results

### 3.1. ADSC Morphology

Overall, there were no observable differences in the morphology of the ADSCs isolated from the well-vascularized and ischemic tissues (Figure 2). The cells of both types were spindle-shaped and elongated with a fibroblastic morphology, a characteristic feature of stem cells.

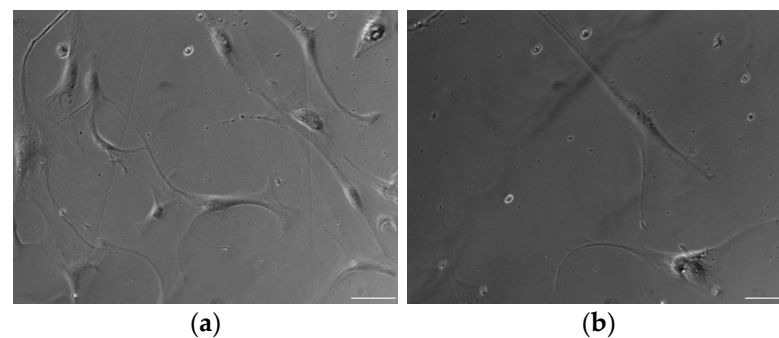


**Figure 2.** Optical microscopy images of ADSCs isolated from (a) well-vascularized and (b) ischemic adipose tissues. Scale bar = 100  $\mu\text{m}$ .

### 3.2. Flow Cytometry

ADSCs isolated from the well-vascularized and ischemic adipose tissues positively immunostained with the conventional mesenchymal stem cell surface markers of CD29, CD44, CD59, CD90, and CD105 (Figure 3). ADSCs isolated from well-vascularized tissues exhibited the following percentage of positive cells for the indicated surface antigens (Figure 3b): CD29 ( $\beta$  1 integrin),  $86.7 \pm 21.9\%$ ; CD44 (hyaluronate receptor),  $98.9 \pm 1.0\%$ ; CD59 (Protectin),  $96.7 \pm 4.0$ ; CD90 (Thy1),  $97.0 \pm 2.8\%$ ; and CD105 (endoglin),  $94.1 \pm 8.0\%$ . The corresponding values for ADSCs isolated from ischemic tissues were CD29,  $78.1 \pm 22.6\%$ ; CD44,  $99.3 \pm 0.4\%$ ; CD59,  $88.7 \pm 9.8$ ; CD90,  $91.7 \pm 8.9\%$ ; and CD105,  $89.3 \pm 11.5\%$ . Both types of ADSCs stained negative with CD31 (PECAM1) and CD106 (VCAM1) markers. A high degree of homogeneity was observed for both positive and negative surface markers on the ADSCs isolated from multiple donors ( $p \leq 0.05$ ). A negligible expression was noted for CD117 (NGFR) and CD271 (LNGFR) for the ADSCs isolated from well-vascularized tissues ( $2.1 \pm 2.1\%$  and  $3.4 \pm 4.2\%$ , respectively) and those isolated from ischemic tissues ( $1.6 \pm 1.3\%$  and  $4.0 \pm 4.8\%$ , respectively). Overall, there were no statistically significant differences ( $p > 0.05$ ) in the abovementioned CD markers between the ADSCs isolated from the well-vascularized and ischemic tissues.

Interestingly, there was a relative change in the CD36 (FAT) marker, which is an integral surface protein involved in fatty acid uptake, for ADSCs isolated from well-vascularized and ischemic tissues of male and female patients (Figure 4). ADSCs isolated from well-vascularized male tissues had  $54.3 \pm 34.6\%$  CD36 positive cells, while the ADSCs isolated from the ischemic male tissues had  $14.6 \pm 14.9\%$  CD36 positive cells. ADSCs isolated from well-vascularized female tissues had  $29.5 \pm 27.4\%$  CD36 positive cells, while the ADSCs isolated from the ischemic female tissues had  $30.3 \pm 14.8\%$  CD36 positive cells (Figure 4a). Furthermore, we calculated the percent change in the CD36 expression of the ADSC isolated from ischemic versus well-vascularized tissues using the following formula:

$$\text{Percent change} = \frac{(\text{CD36 Expression})_{\text{Vascular ADSC}} - (\text{CD36 Expression})_{\text{Ischemic ADSC}}}{(\text{CD36 Expression})_{\text{Vascular ADSC}}} \times 100$$

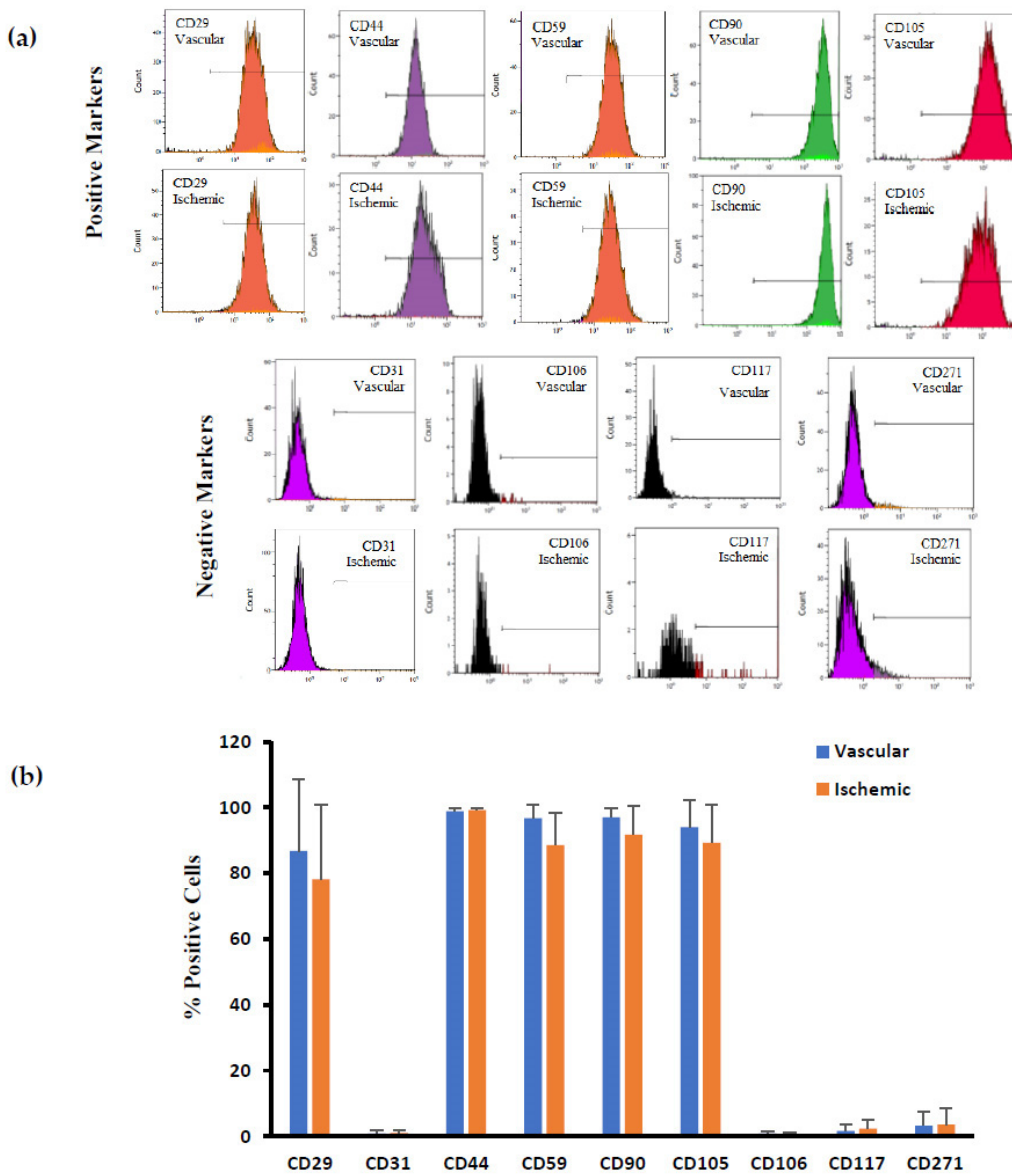


**Figure 3.** (a) Representative flow cytometry histograms of ADSCs isolated from well-vascularized and ischemic adipose tissues. (b) Quantitative measurement of the various CD markers. There were no statistically significant differences ( $p > 0.05$ ) in the CD markers between the ADSCs isolated from the well-vascularized and ischemic tissues.

The percent change in the CD36 expression of the ADSC isolated from ischemic versus well-vascularized tissues for male patients was  $68.9 \pm 30.5\%$  lower while there was no such change for female patients ( $p < 0.05$ ) (Figure 4b).

The stem cell markers for well-vascularized and ischemic tissues for men and women were systematically monitored following spheroid formation (D0 to D3), following 3 days of exposure to cell differentiation media (D3 to M0), and following 10 days of maturation into the adipogenic lineage (M0 to M10) (Figure 5). CD29 expression at D0, M0, and M10 were observed to be  $82.4 \pm 5.4$ ,  $40.8 \pm 15.7$ , and  $25.0 \pm 8.5$ , respectively. CD44 expression at time points D0, M0, and M10 were observed to be  $99.1 \pm 0.5$ ,  $86.1 \pm 6.5$ , and  $80.8 \pm 7.7$ , respectively. CD59 expression at time points D0, M0, and M10 were observed to be  $92.7 \pm 5.5$ ,  $93.3 \pm 3.7$ , and  $91.3 \pm 6.8$ , respectively. CD90 expression at time points D0, M0, and M10 were observed to be  $94.4 \pm 4.7$ ,  $51.0 \pm 26.4$ , and  $52.7 \pm 21.0$ , respectively. CD105 expression at time points D0, M0, and M10 were observed to be  $91.7 \pm 6.9$ ,

14.1 ± 15.0, and 20.5 ± 11.9, respectively. The CD29, CD44, CD90, and CD105 expression on D0 was significantly different from M0 and M10 ( $p \leq 0.05$ ).

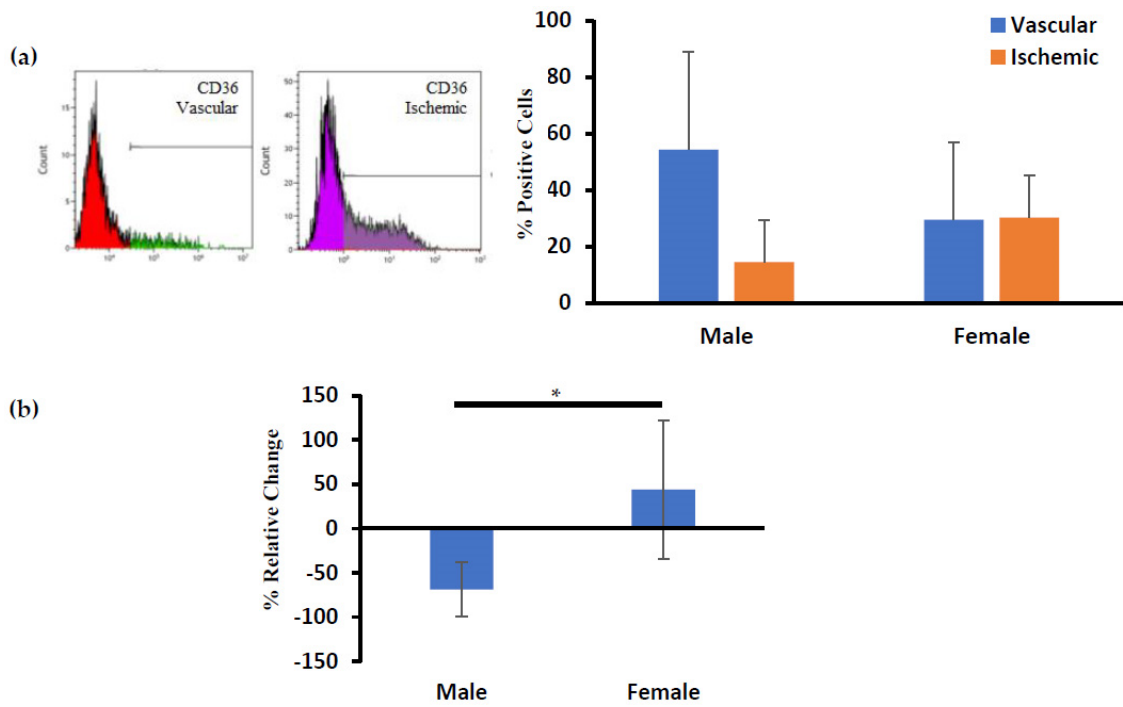


**Figure 4.** (a) Quantitative measurement of CD36 marker for ADSCs isolated from well-vascularized and ischemic adipose tissues of male and female patients. (b) The relative change in the CD36 marker for ADSCs isolated from well-vascularized and ischemic adipose tissues of male and female patients. Error bars indicate 95% confidence intervals. \*  $p \leq 0.05$ .

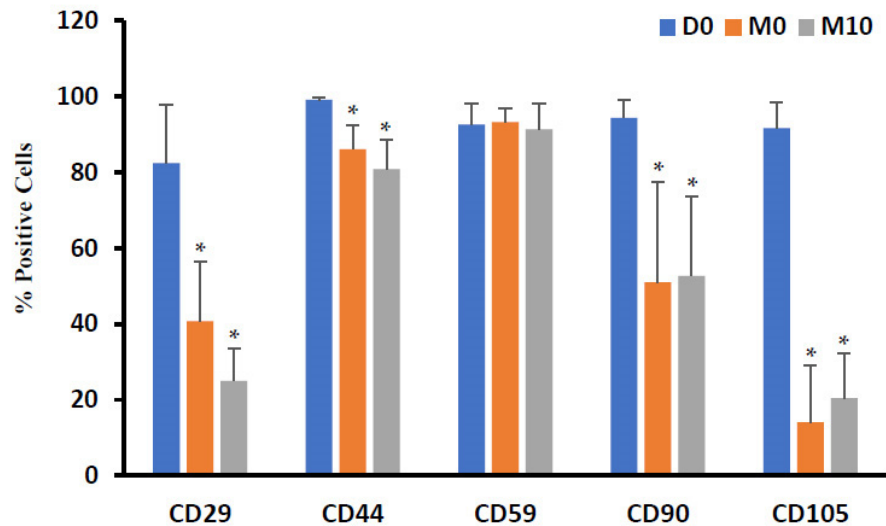


**Figure 5.** Quantitative measurement of various stem CD markers for undifferentiated ADSCs (D0), three-dimensional (3D) spheroid aggregates after 3 days of differentiation (M0) in adipogenic lineage, and ADSCs spheroid differentiated to adipocytes and matured for 10 days (M10). \*  $p \leq 0.05$  compared to D0.

### 3.3. Size Distribution of Differentiated ADSC Spheroids

ADSCs cultured on ELP-PEI coated surfaces formed small three-dimensional (3D) spheroid aggregates during the first 3 days of culture. No significant variation in spheroid

morphology or organization were seen between the spheroids prepared using the ADSCs isolated from the well-vascularized and ischemic tissues (Figure 6a).

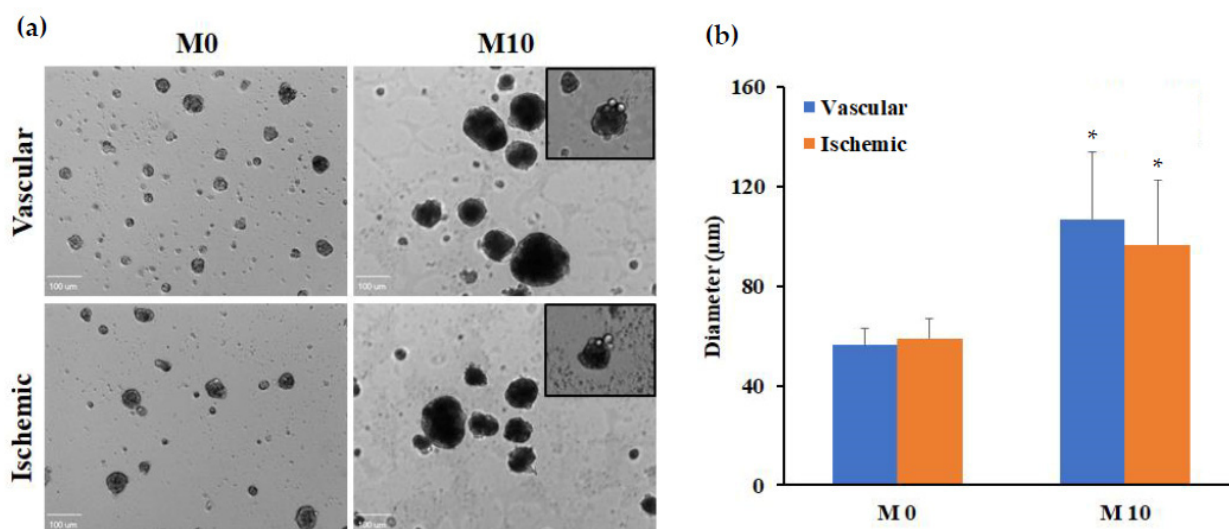


**Figure 6.** Spheroid formation of ADSCs isolated from the well-vascularized and ischemic tissues atop the ELP-PEI coated surface. (a) Bright field morphology, scale bars = 100 μm. The insets show unilocular fat deposits. (b) Quantitative measurement of the ADSC spheroid sizes ( $n > 50$ ). Error bars indicate 95% confidence intervals. \*  $p \leq 0.05$  between M0 and M10 timepoints for the same tissue source.

With an increase in maturation time, the size of the initially formed small spheroids progressively increased, attaining a larger spheroid size by 10 days (M10) in both groups. The adipocyte spheroids after 10 days of maturation mostly had unilocular fat droplets (Figure 6a inset). Measurements taken from micrographs indicated that at the beginning of the maturation phase (M0), spheroids prepared using the ADSCs isolated from the well-vascularized tissues had an average diameter of  $56.3 \pm 6.7 \mu\text{m}$  and the corresponding values for the ADSCs isolated from the ischemic tissues were  $58.8 \pm 7.8 \mu\text{m}$  ( $p > 0.05$ ). These spheroids gradually increased in size to  $106.7 \pm 27.1 \mu\text{m}$  and  $96.6 \pm 26.1 \mu\text{m}$ , respectively, over the 10-day maturation period (Figure 6b;  $p \leq 0.05$  for M10 versus M0 values;  $p > 0.05$  between groups on the same day). Overall, the average spheroid diameter increased ~2-fold over the 10-day maturation period, which is equivalent to a nearly 8-fold increase in the spheroid volume.

### 3.4. Biochemical Characterization

The DNA content decreased significantly in both groups by the end of the 10-day maturation period (Figure 7a). The spheroids prepared using ADSCs isolated from well-vascularized and ischemic tissues had an average DNA content of  $159.6 \pm 31.8 \text{ ng}$  and  $140.5 \pm 28.8 \text{ ng}$ , respectively, on day M0 in maturation media ( $p > 0.05$ ). These DNA content values gradually decreased over 10 days in maturation media to  $85.2 \pm 12.0 \text{ ng}$  and  $68.9 \pm 14.8 \text{ ng}$ , respectively, implying loss of spheroids due to media changes ( $p \leq 0.05$  for M10 versus M0 values;  $p > 0.05$  between groups on the same day). Overall, there were no statistically significant differences ( $p > 0.05$ ) in the average DNA content of the two groups at M0 and M10 days, indicating that the retention of spheroids over the 10-day maturation period was similar in both groups.

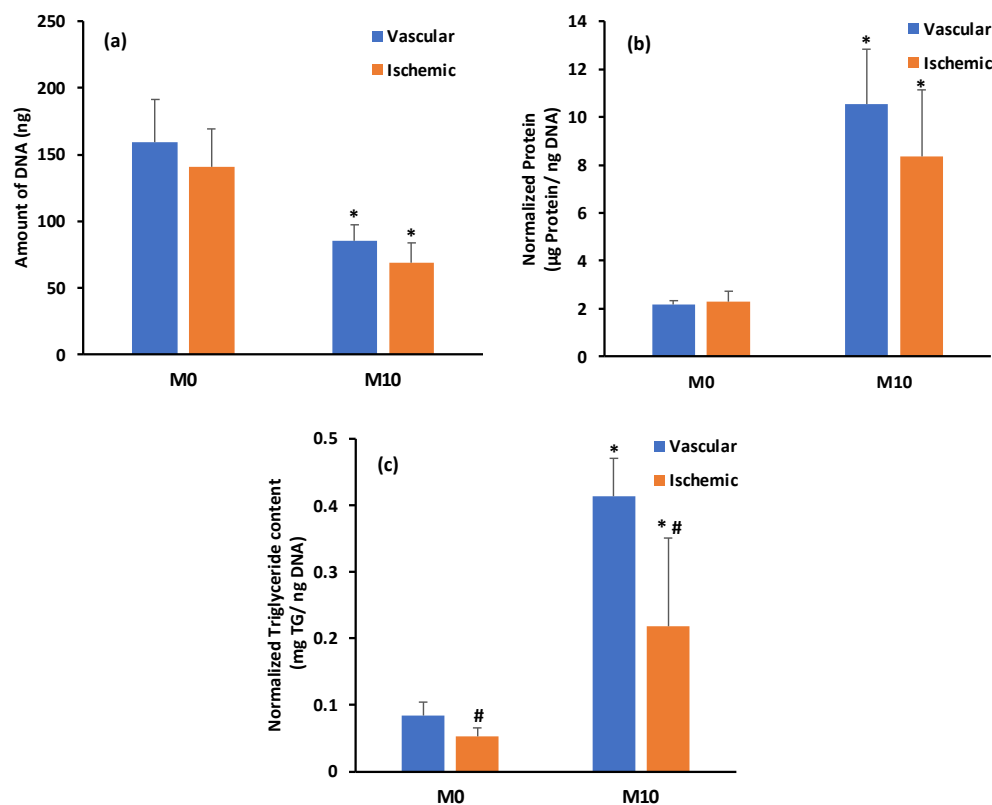


**Figure 7.** (a) DNA quantification; (b) normalized protein content; (c) normalized triglyceride content of spheroids prepared using the ADSCs isolated from the well-vascularized and ischemic tissues after 3 days of differentiation (Day 0 of maturation, M0) and 10 days of maturation (M10). Error bars represent 95% confidence intervals. \*  $p \leq 0.05$  for M10 versus M0 values of the same group; #  $p \leq 0.05$  between groups on the same day.

Protein content normalized to DNA was stable in both groups over the 10-day maturation period (Figure 7b). On day M0, spheroids prepared using the ADSCs isolated from the well-vascularized and ischemic tissues had a normalized protein content of  $2.2 \pm 0.1 \mu\text{g protein/ng DNA}$  and  $2.3 \pm 0.4 \mu\text{g protein/ng DNA}$ , respectively ( $p > 0.05$ ). After 10 days in the maturation media, the average protein content values were  $10.5 \pm 2.3 \mu\text{g protein/ng DNA}$  and  $8.3 \pm 2.8 \mu\text{g protein/ng DNA}$ , respectively ( $p \leq 0.05$  for M10 versus M0 values;  $p > 0.05$  between groups on the same day). Increase in protein content over this period of time indicated the higher metabolic activity of the ADSCs in the spheroid configuration leading to adipogenic maturation.

Triglyceride (TG) content normalized to DNA is indicative of adipogenic differentiation and maturation to adipocytes. In comparison to day M0, both groups accumulated triglycerides over the 10-day maturation period (Figure 7c). The spheroids prepared using the ADSCs isolated from the well-vascularized and ischemic tissues had an average normalized triglyceride content of  $0.08 \pm 0.02 \mu\text{g TG/ng DNA}$  and  $0.05 \pm 0.01 \mu\text{g TG/ng DNA}$ , respectively, on day M0 ( $p \leq 0.05$ ). After 10 days in the maturation media, the average normalized triglyceride content values were  $0.4 \pm 0.1$  and  $0.2 \pm 0.1 \mu\text{g TG/ng DNA}$ , respectively ( $p \leq 0.05$  for M10 versus M0 values;  $p \leq 0.05$  between groups on the same day). Overall, the average normalized triglyceride content increased ~5–6-fold over the 10-day maturation period.

#### 4. Discussion

Increasing evidence indicates that the changing environmental conditions cause changes in ADSCs response to proliferation, differentiation, migration, lipogenesis, and apoptotic susceptibility [31]. Here, we investigated if ADSCs from adipose tissue under

ischemic conditions undergo dysfunctional alterations generating unique immunophenotypic profile and subsequent adipogenic differentiation compared with the ADSCs from a well-vascularized environment. Flow cytometry analysis of cell surface markers is an excellent technique to determine and differentiate between the type of cells isolated and to identify the expressed surface antigens that may have downstream functionality. This is the first study that examines differences in surface marker expression for ADSCs isolated under well-vascularized and ischemic conditions from same individuals. This identification and analysis are particularly relevant because these cells are a promising tool for cellular regenerative therapies, and the variation in surface antigen expression due to environmental or related factors may cause different protein expression on these cells, which may affect their usability in regenerative medicine.

Benefits of 3D aggregates or spheroids over 2D monolayer cultures has been thoroughly investigated in recent times and results show increased expression of adipose-specific genes like PPAR- $\gamma$ , CCAAT/enhancer-binding protein (C/EBP- $\alpha$ ), and adiponectin along with enhanced triglyceride accumulation [32–34]. Moreover, 3D spheroids of adipocytes represent similar morphological character as seen in native adipose tissue. We have previously shown that cells seeded atop an ELP-PEI surface adopted spheroidal configuration and the cells better expressed lineage specific markers compared to 2D culture systems [4,6,30]. Our lab has shown that spheroid culture improves metabolic profile compared to typical monolayer cultures and spheroid growth correlates to better function [16,30]. In this study, we seeded the ADSCs on an ELP-PEI coated surface to induce them to form 3D spheroids and allow the cells to differentiate toward the adipocyte lineage. The cells isolated from well-vascularized and ischemic adipose tissues were analyzed per the guidelines set by the International Society for Cellular Therapy (ISCT) for stem cell identification and were confirmed to be ADSCs [35]. In our study, a similar positive expression profile for ADSC surface markers CD29, CD44, CD59, CD90, and CD105 was observed when compared to Zavan et al., Pachón-Peña et al., and Tucker et al. (Figure 3) [31,36,37]. A similar profile for the mesenchymal stem cells markers was also observed by De Francesco et al. for nonenzymatically extracted adipose derived stem cells [38]. While the isolated ADSCs on D0 expressed significant amount of CD29, CD44, CD59, CD90, and CD105, differentiation and maturation of the ADSCs along the adipogenic lineage resulted in significant reduction in the expression CD29, CD44, CD90, and CD105 (Figure 5). CD29 or integrin  $\beta$ 1 is involved in the interaction of cells with the ECM proteins such as collagen, laminin, and fibronectin. CD44 is a type I transmembrane glycoprotein that binds hyaluronic acid (HA) in most cell types, which later plays a role in cell migration, cell–cell, and cell–matrix adhesion. CD90 or Thy-1 is a cell surface protein widely used as a stem cell marker that has speculated roles in cell–cell and cell–matrix interactions. As these CD stem cell markers play a major role in cell adhesion, the decrease in their expression can be contributed to either the formation of spheroids or differentiation of ADSCs to adipogenic lineage. CD59 is membrane bound glycoprotein that regulates complement mediated cell lysis. As reported by Festy et al., CD59 is homogeneously expressed by both precursor cell and mature adipocytes [39]. The similar expression of CD59 by both ADSCs on D0 and mature adipocytes on M10, thus agrees with Festy et al. CD105 (endoglin) is a type I membrane glycoprotein that functions as a receptor for TGF-beta ligands and is highly expressed in vascular endothelial cells. Interestingly, MSCs isolated from the adipose tissue have been shown to express CD105 at low levels when freshly isolated but become increasingly CD105+ upon culture passages.

Our results for negative expression of CD31 also matches with Huang et al. and confirms absence of endothelial cells [40]. Calabrese et al. and Mifune et al. reported that the proliferation efficiency and trilineage differentiation of CD271+ stem cells isolated from adipose tissue is higher than those isolated from bone marrow [41,42]. Kohli et al. also illustrated that CD271+ MSCs significantly accelerated osteochondral wound healing with reduced vascularization when injected into athymic mice [43]. We found that the proportion of CD271+ cells were low, but similar in ischemic tissue compared to well-vascularized

tissue (Figure 3). Recently, ISCT and International Federation for Adipose Therapeutics and Science (IFATS) have put forward additional markers for ADSC identification; positive expression profile for CD36 and negative for CD106 that clearly distinguishes them from bone marrow MSCs [44]. ADSCs isolated under the well-vascularized and ischemic conditions fit into this category because they were CD36 positive and CD106 negative (Figures 3 and 4).

Currently, there are no FDA-approved anti-obesity drugs on the market that directly target the adipose tissue [26]. To identify an optimal drug candidate, an *in vitro* adipocyte model must closely mimic *in vivo* tissue structure. These models will provide insights into fat absorption, metabolism, and lipolysis mechanisms, aiding in the identification of promising drug candidates for further testing. These advancements not only decrease dependence on animal testing but also pave the way for innovative approaches to targeting adipocyte responses. Therefore, we differentiated the ADSCs isolated from well-vascularized and ischemic samples into adipocytes. The spheroids prepared using the ADSCs isolated from the well-vascularized and ischemic tissues showed a significant increase in size as well as lipid accumulation over the 10-day maturation period, suggesting their successful differentiation to adipocytes (Figures 6 and 7). However, spheroids prepared using the ADSCs isolated from the ischemic tissues had a lower triglyceride content compared to the spheroids prepared using the ADSCs isolated from the well-vascularized tissues (Figure 7c). The behavior of the spheroids prepared using the ADSCs isolated from the ischemic tissues during 10 days of adipogenic maturation (lower triglyceride content) may be due to the ischemic/hypoxia condition experienced during the surgical harvest of the ADSCs, which may induce a more long-term metabolic dysfunction resulting in a less efficient commitment to follow adipogenic differentiation and, therefore, less effective fatty acids uptake and intracellular lipid metabolism. One such trigger may be the CD36-dependent autophagic pathway that maintains the cell homeostasis. It is well known that CD36 promotes the fatty acid uptake in adipocytes and other differentiated cells. However, little is currently known about the role of CD36 in multipotent undifferentiated ADSCs isolated from ischemic tissues. CD36 is a multiligand receptor contributing to glucose and lipid metabolism, immune response, inflammation, thrombosis, and fibrosis [45]. CD36 is also associated with macrophage foam cell development in atheromatous plaque formation, insulin resistance, oxidative stress (i.e., ischemia-reperfusion injury), and apoptosis/autophagy mechanisms [46]. Within CD36 functions, the CD36-dependent autophagic pathway is a cell survival mechanism that regulates cell homeostasis by modulating the mitochondrial dysfunction under ischemic conditions [47]. Consistent with these facts, it is not unreasonable to postulate that, in our ADSCs isolated from the ischemic tissues, the lower expression of CD36 plays a role in achieving the lower triglyceride content after 10 days of adipogenic maturation and the lower triglyceride content may be the result of increasing fatty acids catabolism to satisfy energy demands of the intracellular stress and therefore protect cells from apoptosis.

Limitations of our study include the relatively small number of samples used. We acknowledge that the limited sample size may impact the generalizability of our findings and the statistical power of our analyses. Additionally, assessments comprising of comparing cellular proliferation rates, determining ADSC yield from different types of adipose tissue, and evaluating multipotency through differentiation into osteocytes and cartilage cells will be valuable for a comprehensive understanding of ADSC characteristics. Even with these limitations, the implications of these findings for clinical practice are profound. This study will help develop a better understanding of the impact of tissue ischemia on ADSC functionality and could help in developing surgical strategies for adipose tissue harvesting. By optimization of tissue harvesting conditions to preserve tissue vascularity and minimize ischemic injury, clinicians may enhance the quality and functionality of isolated ADSCs for subsequent therapeutic applications. Furthermore, interpreting the molecular mechanisms underlying the observed functional differences may help develop interventions to improve ADSC function in ischemic conditions. This information could be

used as a guide for development of novel strategies to enhance adipose tissue engineering and regenerative medicine approaches.

## 5. Conclusions

In this study, we compared variations in immunophenotypes and functionalities of ADSCs isolated from adipose tissues harvested within the first 5 min of the initial surgical incision, which is considered a well-vascularized, nonpremedicated condition versus tissues obtained after the ALT flaps were fully harvested and are from the more distal part of the flaps where the blood supply was considered deprived. The isolated ADSCs were confirmed to be mesenchymal stem cells. The ADSCs were cultured as 3D spheroids and after 10 days showed a significant increase in size as well as lipid accumulation, suggesting their successful differentiation to adipocytes. However, the spheroids formed using the ADSCs isolated from ischemic adipose tissue had a lower triglyceride content compared to those formed using the ADSCs isolated from the well-vascularized tissue. These results indicate that the ADSCs isolated from ischemic tissues either fail to uptake fatty acids or fail to efficiently convert those fatty acids into triglycerides. Elucidating the role of high CD36 expression in ischemic ADSCs may reinforce our hypothesis that the harvest of adipose tissues in well-vascularized and nonpremedicated conditions will yield the isolation of healthier ADSCs.

**Author Contributions:** Conceptualization, A.V.J. and A.M.; methodology, A.V.J., A.M., J.S.S., J.M.P. and P.P.; formal analysis, P.P., S.C., C.A.C., R.B. and J.M.P.; investigation, P.P., S.C., C.A.C., R.B. and J.M.P.; resources, A.V.J., A.M., J.S.S. and B.M.; writing—original draft preparation, P.P.; writing—review and editing, A.V.J., A.M., J.S.S., J.M.P., P.P., S.C., C.A.C., R.B. and B.M.; visualization, P.P. and S.C.; supervision, A.V.J.; project administration, A.V.J.; funding acquisition, A.V.J. and A.M. All authors have read and agreed to the published version of the manuscript.

**Funding:** This work was funded in part by the National Institutes of Health (NIH; R01EB020006 and R01DK124327 awarded to A.V.J. and J.S.S., respectively) and an intramural grant awarded to A.M. by the UMMC Cardiorenal and Metabolic Diseases Research Center under a parent grant from the National Institutes of Health (NIH; P20GM104357). The UMMC Cancer Center and Research Institute Flow Cytometry Core Facility is supported in part through the UMMC Mississippi Center of Excellence in Perinatal Research (MS-CEPR)-COBRE (P20GM121334).

**Institutional Review Board Statement:** This study was approved by the Institutional Review Board of the University of Mississippi Medical Center (# 2012-0004).

**Informed Consent Statement:** Patient consent was waived due to the use of medically discarded tissues.

**Data Availability Statement:** The data presented in this study are available on request from the corresponding author.

**Acknowledgments:** This work made use of equipment available in the Department of Biomedical Materials Science Shared Equipment Facility.

**Conflicts of Interest:** The authors have no conflicts of interest to declare.

## References

1. Cercato, C.; Fonseca, F.A. Cardiovascular risk and obesity. *Diabetol. Metab. Syndr.* **2019**, *11*, 74. [[CrossRef](#)] [[PubMed](#)]
2. Kelly, T.; Yang, W.; Chen, C.S.; Reynolds, K.; He, J. Global burden of obesity in 2005 and projections to 2030. *Int. J. Obes.* **2008**, *32*, 1431–1437. [[CrossRef](#)] [[PubMed](#)]
3. Zhu, X.Y.; Ma, S.; Eirin, A.; Woollard, J.R.; Hickson, L.J.; Sun, D.; Lerman, A.; Lerman, L.O. Functional plasticity of adipose-derived stromal cells during development of obesity. *Stem Cells Transl. Med.* **2016**, *5*, 893–900. [[CrossRef](#)] [[PubMed](#)]
4. Gurumurthy, B.; Bierdeman, P.C.; Janorkar, A.V. Spheroid model for functional osteogenic evaluation of human adipose derived stem cells. *J. Biomed. Mater. Res. A* **2017**, *105*, 1230–1236. [[CrossRef](#)] [[PubMed](#)]
5. Stromps, J.P.; Paul, N.E.; Rath, B.; Nourbakhsh, M.; Bernhagen, J.; Pallua, N. Chondrogenic differentiation of human adipose-derived stem cells: A new path in articular cartilage defect management? *BioMed Res. Int.* **2014**, *2014*, 1–7. [[CrossRef](#)] [[PubMed](#)]
6. Turner, P.A.; Gurumurthy, B.; Bailey, J.L.; Elks, C.M.; Janorkar, A.V. Adipogenic differentiation of human adipose-derived stem cells grown as spheroids. *Process Biochem.* **2017**, *59*, 312–320. [[CrossRef](#)] [[PubMed](#)]

7. Kaisang, L.; Siyu, W.; Lijun, F.; Daoyan, P.; Xian, C.J.; Jie, S. Adipose-derived stem cells seeded in Pluronic F-127 hydrogel promotes diabetic wound healing. *J. Surg. Res.* **2017**, *217*, 63–74. [[CrossRef](#)] [[PubMed](#)]
8. Zhang, P.; Feng, J.; Liao, Y.; Cai, J.; Zhou, T.; Sun, M.; Gao, J.; Gao, K. Ischemic flap survival improvement by composition-selective fat grafting with novel adipose tissue derived product—Stromal vascular fraction gel. *Biochem. Biophys. Res. Commun.* **2018**, *495*, 2249–2256. [[CrossRef](#)] [[PubMed](#)]
9. Arslan, F.; Lai, R.C.; Smeets, M.B.; Akeroyd, L.; Choo, A.; Agur, E.N.; Timmers, L.; van Rijen, H.V.; Doevendans, P.A.; Pasterkamp, G.; et al. Mesenchymal stem cell-derived exosomes increase ATP levels, decrease oxidative stress and activate PI3K/Akt pathway to enhance myocardial viability and prevent adverse remodeling after myocardial ischemia/reperfusion injury. *Stem Cell Res.* **2013**, *10*, 301–312. [[CrossRef](#)]
10. Eyuboglu, A.A.; Uysal, C.A.; Ozgun, G.; Coskun, E.; Markal Ertas, N.; Haberal, M. The effect of adipose derived stromal vascular fraction on stasis zone in an experimental burn model. *Burns* **2018**, *44*, 386–396. [[CrossRef](#)]
11. Jin, E.; Chae, D.S.; Son, M.; Kim, S.W. Angiogenic characteristics of human stromal vascular fraction in ischemic hindlimb. *Int. J. Cardiol.* **2017**, *234*, 38–47. [[CrossRef](#)] [[PubMed](#)]
12. Lin, K.C.; Yip, H.K.; Shao, P.L.; Wu, S.C.; Chen, K.H.; Chen, Y.T.; Yang, C.C.; Sun, C.K.; Kao, G.S.; Chen, S.Y.; et al. Combination of adipose-derived mesenchymal stem cells (ADMSC) and ADMSC-derived exosomes for protecting kidney from acute ischemia-reperfusion injury. *Int. J. Cardiol.* **2016**, *216*, 173–185. [[CrossRef](#)] [[PubMed](#)]
13. Pu, C.M.; Liu, C.W.; Liang, C.J.; Yen, Y.H.; Chen, S.H.; Jiang-Shieh, Y.F.; Chien, C.L.; Chen, Y.C.; Chen, Y.L. Adipose-derived stem cells protect skin flaps against ischemia/reperfusion injury via IL-6 expression. *J. Investig. Dermatol.* **2017**, *137*, 1353–1362. [[CrossRef](#)] [[PubMed](#)]
14. Bajek, A.; Gurtowska, N.; Olkowska, J.; Maj, M.; Kaźmierski, L.; Bodnar, M.; Marszałek, A.; Dębski, R.; Drewna, T. Does the harvesting technique affect the properties of adipose-derived stem cells? The comparative biological characterization. *J. Cell. Biochem.* **2017**, *118*, 1097–1107. [[CrossRef](#)] [[PubMed](#)]
15. Rodbell, M. Metabolism of isolated fat cells. I. Effects of hormones on glucose metabolism and lipolysis. *J. Biol. Chem.* **1964**, *239*, 375–380. [[CrossRef](#)]
16. Palumbo, P.; Lombardi, F.; Siragusa, G.; Cifone, M.G.; Cinque, B.; Giuliani, M. Methods of isolation, characterization and expansion of human adipose-derived stem cells (ASCs): An overview. *Int. J. Mol. Sci.* **2018**, *19*, 1897. [[CrossRef](#)] [[PubMed](#)]
17. Baer, P.C.; Geiger, H. Adipose-derived mesenchymal stromal/stem cells: Tissue localization, characterization, and heterogeneity. *Stem Cells Int.* **2012**, *2012*, 1–11. [[CrossRef](#)] [[PubMed](#)]
18. Casteilla, L.; Planat-Benard, V.; Laharrague, P.; Cousin, B. Adipose-derived stromal cells: Their identity and uses in clinical trials, an update. *World J. Stem Cells* **2011**, *3*, 25–33. [[CrossRef](#)]
19. Mitchell, J.B.; McIntosh, K.; Zvonick, S.; Garrett, S.; Floyd, Z.E.; Kloster, A.; Di Halvorsen, Y.; Storms, R.W.; Goh, B.; Kilroy, G.; et al. Immunophenotype of human adipose-derived cells: Temporal changes in stromal-associated and stem cell-associated markers. *Stem Cells* **2006**, *24*, 376–385. [[CrossRef](#)]
20. Phinney, D.G.; Sensebé, L. Mesenchymal stromal cells: Misconceptions and evolving concepts. *Cytotherapy* **2013**, *15*, 140–145. [[CrossRef](#)]
21. Varma, M.J.; Breuls, R.G.; Schouten, T.E.; Jurgens, W.J.; Bontkes, H.J.; Schuurhuis, G.J.; van Ham, S.M.; van Milligen, F.J. Phenotypical and functional characterization of freshly isolated adipose tissue-derived stem cells. *Stem Cells Dev.* **2007**, *16*, 91–104. [[CrossRef](#)] [[PubMed](#)]
22. Ylöstalo, J.; Bazhanov, N.; Prockop, D.J. Reversible commitment to differentiation by human multipotent stromal cells in single-cell-derived colonies. *Exp. Hematol.* **2008**, *36*, 1390–1402. [[CrossRef](#)] [[PubMed](#)]
23. Goldman, J.J.; Wang, W.Z.; Fang, X.H.; Williams, S.J.; Baynosa, R.C. Tumescence Liposuction without Lidocaine. *Plast. Reconstr. Surg. Glob. Open* **2016**, *4*, e829. [[CrossRef](#)]
24. Nie, H.; Kubrova, E.; Wu, T.; Denbeigh, J.M.; Hunt, C.; Dietz, A.B.; Smith, J.; Qu, W.; van Wijnen, A.J. Effect of lidocaine on viability and gene expression of human adipose-derived mesenchymal stem cells: An in vitro study. *PM R* **2019**, *11*, 1218–1227. [[CrossRef](#)] [[PubMed](#)]
25. Wu, T.; Shi, Z.; Song, H.; Li, Y.; Li, J.H. Cytotoxicity of local anesthetics on rabbit adipose-derived mesenchymal stem cells during early chondrogenic differentiation. *Exp. Ther. Med.* **2018**, *16*, 2843–2850. [[CrossRef](#)] [[PubMed](#)]
26. NIDDK Website. Available online: <https://www.niddk.nih.gov/health-information/weight-management/prescription-medications-treat-overweight-obesity> (accessed on 18 April 2024).
27. Clinicaltrials.gov Website. Available online: <https://clinicaltrials.gov/ct2/results?cond=Obesity&term=&cntry=&state=&city=&dist=> (accessed on 18 April 2024).
28. Adan, R.A.H. Mechanisms underlying current and future anti-obesity drugs. *Trends Neurosci.* **2013**, *36*, 133–140. [[CrossRef](#)] [[PubMed](#)]
29. Colon-Gonzalez, F.; Kim, G.W.; Lin, J.E.; Valentino, M.A.; Waldman, S.A. Obesity pharmacotherapy: What is next? *Mol. Asp. Med.* **2013**, *34*, 71–83. [[CrossRef](#)] [[PubMed](#)]
30. Turner, P.A.; Harris, L.M.; Purser, C.A.; Baker, R.C.; Janorkar, A.V. A surface-tethered spheroid model for functional evaluation of 3T3-L1 adipocytes. *Biotechnol. Bioeng.* **2014**, *111*, 174–183. [[CrossRef](#)]

31. Pachón-Peña, G.; Serena, C.; Ejarque, M.; Petriz, J.; Duran, X.; Oliva-Olivera, W.; Simó, R.; Tinahones, F.J.; Fernández-Veledo, S.; Vendrell, J. Obesity determines the immunophenotypic profile and functional characteristics of human mesenchymal stem cells from adipose tissue. *Stem Cells Transl. Med.* **2016**, *5*, 464–475. [[CrossRef](#)]
32. Bhang, S.H.; Lee, S.; Shin, J.Y.; Lee, T.J.; Kim, B.S. Transplantation of cord blood mesenchymal stem cells as spheroids enhances vascularization. *Tissue Eng. Part A* **2012**, *18*, 2138–2147. [[CrossRef](#)]
33. Cheng, N.C.; Wang, S.; Young, T.H. The influence of spheroid formation of human adipose-derived stem cells on chitosan films on stemness and differentiation capabilities. *Biomaterials* **2012**, *33*, 1748–1758. [[CrossRef](#)] [[PubMed](#)]
34. Miyagawa, Y.; Okita, H.; Hiroyama, M.; Sakamoto, R.; Kobayashi, M.; Nakajima, H.; Katagiri, Y.U.; Fujimoto, J.; Hata, J.; Umezawa, A.; et al. A microfabricated scaffold induces the spheroid formation of human bone marrow-derived mesenchymal progenitor cells and promotes efficient adipogenic differentiation. *Tissue Eng. Part A* **2011**, *17*, 513–521. [[CrossRef](#)] [[PubMed](#)]
35. Dominici, M.; Le Blanc, K.; Mueller, I.; Slaper-Cortenbach, I.; Marini, F.; Krause, D.; Deans, R.; Keating, A.; Prockop, D.; Horwitz, E. Minimal criteria for defining multipotent mesenchymal stromal cells. The International Society for Cellular Therapy position statement. *Cytotherapy* **2006**, *8*, 315–317. [[CrossRef](#)] [[PubMed](#)]
36. Tucker, H.A.; Bunnell, B.A. Characterization of human adipose-derived stem cells using flow cytometry. *Methods Mol. Biol.* **2011**, *702*, 121–311. [[PubMed](#)]
37. Zavan, B.; Giorgi, C.; Bagnara, G.P.; Vindigni, V.; Abatangelo, G.; Cortivo, R. Osteogenic and chondrogenic differentiation: Comparison of human and rat bone marrow mesenchymal stem cells cultured into polymeric scaffolds. *Eur. J. Histochem.* **2007**, *51*, 1–8. [[PubMed](#)]
38. De Francesco, F.; Riccio, V.; Biswas, R.; Busato, A.; Di Bella, C.; Serri, E.; Sbarbati, A.; Zavan, B.; Riccio, M.; Palumbo Piccionello, A. *In Vitro* Characterization of canine microfragmented adipose tissue non-enzymatically extracted from the thigh and lumbar regions. *Animals* **2021**, *11*, 3231. [[CrossRef](#)] [[PubMed](#)]
39. Festy, F.; Hoareau, L.; Bes-Houtmann, S.; Péquin, A.M.; Gonthier, M.P.; Munstun, A.; Hoarau, J.J.; Césari, M.; Roche, R. Surface protein expression between human adipose tissue-derived stromal cells and mature adipocytes. *Histochem. Cell Biol.* **2005**, *124*, 113–121. [[CrossRef](#)] [[PubMed](#)]
40. Huang, S.J.; Fu, R.H.; Shyu, W.C.; Liu, S.P.; Jong, G.P.; Chiu, Y.W.; Wu, H.S.; Tsou, Y.A.; Cheng, C.W.; Lin, S.Z. Adipose-derived stem cells: Isolation, characterization, and differentiation potential. *Cell Transplant.* **2013**, *22*, 701–709. [[CrossRef](#)] [[PubMed](#)]
41. Calabrese, G.; Giuffrida, R.; Lo Furno, D.; Parrinello, N.L.; Forte, S.; Gulino, R.; Colarossi, C.; Schinocca, L.R.; Giuffrida, R.; Cardile, V.; et al. Potential effect of CD271 on human mesenchymal stromal cell proliferation and differentiation. *Int. J. Mol. Sci.* **2015**, *16*, 15609–15624. [[CrossRef](#)]
42. Mifune, Y.; Matsumoto, T.; Murasawa, S.; Kawamoto, A.; Kuroda, R.; Shoji, T.; Kuroda, T.; Fukui, T.; Kawakami, Y.; Kurosaka, M.; et al. Therapeutic superiority for cartilage repair by CD271-positive marrow stromal cell transplantation. *Cell Transplant.* **2013**, *22*, 1201–1211. [[CrossRef](#)]
43. Kohli, N.; Al-Delfi, I.R.T.; Snow, M.; Sakamoto, T.; Miyazaki, T.; Nakajima, H.; Uchida, K.; Johnson, W.E.B. CD271-selected mesenchymal stem cells from adipose tissue enhance cartilage repair and are less angiogenic than plastic adherent mesenchymal stem cells. *Sci. Rep.* **2019**, *9*, 3194. [[CrossRef](#)] [[PubMed](#)]
44. Bourin, P.; Bunnell, B.A.; Casteilla, L.; Dominici, M.; Katz, A.J.; March, K.L.; Redl, H.; Rubin, J.P.; Yoshimura, K.; Gimble, J.M. Stromal cells from the adipose tissue-derived stromal vascular fraction and culture expanded adipose tissue-derived stromal/stem cells: A joint statement of the International Federation for Adipose Therapeutics and Science (IFATS) and the International Society for Cellular Therapy (ISCT). *Cytotherapy* **2013**, *15*, 641–648.
45. Puchałowicz, K.; Rać, M.E. The multifunctionality of CD36 in diabetes mellitus and its complications-update in pathogenesis, treatment and monitoring. *Cells* **2020**, *9*, 1877. [[CrossRef](#)] [[PubMed](#)]
46. Yang, M.; Silverstein, R.L. CD36 and ERK5 link dyslipidemia to apoptotic-like platelet procoagulant function. *Curr. Opin. Hematol.* **2019**, *26*, 357–365. [[CrossRef](#)] [[PubMed](#)]
47. Chen, Y.; Yang, M.; Huang, W.; Chen, W.; Zhao, Y.; Schulte, M.L.; Volberding, P.; Gerbec, Z.; Zimmermann, M.T.; Zeighami, A.; et al. Mitochondrial metabolic reprogramming by CD36 signaling drives macrophage inflammatory responses. *Circ. Res.* **2019**, *125*, 1087–1102. [[CrossRef](#)]

**Disclaimer/Publisher’s Note:** The statements, opinions and data contained in all publications are solely those of the individual author(s) and contributor(s) and not of MDPI and/or the editor(s). MDPI and/or the editor(s) disclaim responsibility for any injury to people or property resulting from any ideas, methods, instructions or products referred to in the content.